Two-dimensional differential in-gel electrophoresis–based proteomics of male gametes in relation to oxidative stress

Alaa Hamada, M.D.,[a] Rakesh Sharma, Ph.D.,[a] Stefan S. du Plessis, Ph.D.,[d] Belinda Willard, Ph.D.,[b] Satya P. Yadav, Ph.D.,[c] Edmund Sabanegh, M.D.,[a] and Ashok Agarwal, Ph.D.[a]

[a] Center for Reproductive Medicine, Glickman Urological and Kidney Institute; [b] Proteomics Core Services; [c] Molecular Biotechnology, Lerner Research Institute, Cleveland Clinic, Cleveland, Ohio; and [d] Medical Physiology, Stellenbosch University, Tygerberg, South Africa

Objective: To identify the relative abundance of proteins in pooled reactive oxygen species (ROS)–positive (ROS+) and ROS-negative (ROS−) semen samples with the use of two-dimensional differential in-gel electrophoresis (2D-DIGE).
Design: Spermatozoa suspensions from ROS+ and ROS− groups by 2D-DIGE analysis.
Setting: Tertiary hospital.
Patient(s): 20 donors and 32 infertile men.
Intervention(s): Seminal ejaculates evaluated for semen and proteomic analysis.
Main Outcome Measure(s): Semen samples from 20 donors and 32 infertile men were pooled, divided into ROS+ and ROS− groups based on the cutoff value of <20 relative light units/s/10^6 sperm and frozen. From each pooled group, spermatozoa were labeled with Cy3/Cy5 fluorescent dye. Duplicate 2D-DIGE gels were run. Image analysis was performed with the use of Decider software. Protein spots exhibiting ≥ 1.5-fold difference in intensity were excised from the preparatory gel and identified by liquid chromatography–mass spectrometry. Data were analyzed with the use of Sequest and Blast programs.
Result(s): A total of 1,343 protein spots in gel 1 (ROS−) and 1,265 spots in gel 2 (ROS+) were detected. The majority of protein spots had similar expression, with 31 spots were differentially expressed. Six spots were significantly decreased and 25 increased in the ROS− sample compared with the ROS+ sample.
Conclusion(s): Significantly different expression of protective proteins against oxidative stress was found in ROS−compared with ROS+ samples. These differences may explain the role of oxidation species in the pathology of male infertility. (Fertil Steril® 2013;99:1216–26. ©2013 by American Society for Reproductive Medicine.)
Key Words: Spermatozoa, reactive oxygen species, proteomics, electrophoresis, mass spectroscopy, male infertility, oxidative stress

Discuss: You can discuss this article with its authors and with other ASRM members at http://fertstertforum.com/hamadaa-electrophoresis-proteomics-spermatozoa/

Use your smartphone to scan this QR code and connect to the discussion forum for this article now.*

* Download a free QR code scanner by searching for "QR scanner" in your smartphone's app store or app marketplace.

An elevated level of reactive oxygen species (ROS) is reported in 40%–88% of infertile men (1); however, there is a paucity of information about the exact mechanisms that generate or protect against ROS. ROS are oxygen-derived reactive molecules with short half-lives, formed as byproducts of normal cellular oxygen metabolism to regulate cellular homeostasis and cell signaling (2). They are categorized into free radicals, i.e., molecules with one or more unpaired electrons, such as superoxide anion ($O2-\bullet$) hydroxyl radical ($OH\cdot$), and the hypochlorite ion (OCl^-), and nonradical molecules such as the powerful oxidant H_2O_2. There are two common forms of free radicals, namely, ROS and reactive nitrogen species (RNS), which are a subclass of ROS, e.g., nitric oxide (NO), nitrous oxide (N_2O), peroxynitrite

Received July 10, 2012; revised November 7, 2012; accepted November 26, 2012; published online January 8, 2013.
A.H. has nothing to disclose. R.S. has nothing to disclose. S.S.d.P. has nothing to disclose. B.W. has nothing to disclose. S.P.Y. has nothing to disclose. E.S. has nothing to disclose. A.A. has nothing to disclose.
Presented at the 68th American Society for Reproductive Medicine, San Diego, California, October 20–24, 2012.
Reprint requests: Ashok Agarwal, Ph.D., Glickman Urological and Kidney Institute, Cleveland Clinic, 9500 Euclid Avenue, Desk A19, Cleveland, Ohio 44195 (E-mail: agarwaa@ccf.org).

Fertility and Sterility® Vol. 99, No. 5, April 2013 0015-0282/$36.00

http://dx.doi.org/10.1016/j.fertnstert.2012.11.046

($ONOO^-$) nitroxyl (HNO), and peroxynitrous acid (HNO_3) (3, 4). Antioxidants act as free radical scavengers. They help to maintain the homeostatic levels of free radicals and physiologic functions and to prevent pathologic effects as a result of oxidative stress (OS) (5).

Free radicals regulate sperm maturation, capacitation and hyperactivation, acrosome reaction (AR), and sperm-oocyte fusion (6–8). At toxic levels, these highly reactive molecules attack the nearest valent-stable molecule to obtain an electron. Subsequently, the targeted molecule becomes a free radical itself and initiates a cascade of events that can ultimately lead to cellular damage (5). ROS induce protein damage, lipid peroxidation (LPO), apoptosis, and DNA damage (9, 10).

Spermatozoa are distinctively susceptible to OS because of limited cytoplasmic antioxidants and high plasma membrane content of polyunsaturated fatty acids (PUFA) that are susceptible to LPO. LPO may result in membrane permeabilization, causing an efflux of adenosine triphosphate necessary for flagellar movement (11, 12). OS can further affect sperm function by impairing the viability, motility, and fertilization potential of spermatozoa (13–16).

Advances in proteomics, which is the study of the protein profile of a particular cell or tissue, has helped increase our understanding of the structural and functional proteins present in the spermatozoa and seminal plasma. Proteomics allows a wider view of investigating the oxidative stress response than the conventional biochemical methods (17). Proteomic studies also demonstrate the oxidative stress component in a variety of complex cellular processes, including cell signaling, aging, and various other pathologies. Proteomic analysis has also shown that modification of several peroxiredoxins that are enzymes catalyzing the destruction of peroxides is a major cellular response to oxidative stress (18). Proteomic techniques, such as two-dimensional differential in-gel electrophoresis (2D-DIGE) and polyacrylamide gel electrophoresis (2D-PAGE), coupled with mass spectrometry (MS), have allowed for the identification of numerous sperm-specific proteins. These approaches can recognize proteins involved in particular sperm processes, such as motility, capacitation, acrosome reaction, and fertilization. Studies of the sperm proteome have demonstrated how post-translational modifications, such as phosphorylation, glycosylation, proteolytic cleavage, and mutations, bring about the physiologic changes in spermatozoa function (19–21). Furthermore, proteomic analysis, by measuring the differential expression of proteins, has allowed for the study of spermatozoa in different functional states—immature versus mature, uncapacitated versus capacitated, normal versus defective, and low sperm count versus high sperm count—all of which affect the male reproductive potential (21).

Differences in the levels of spermatozoal protein expression under oxidative stress may be related to: 1) effect of OS on genes inducing or inhibiting particular protein synthesis; 2) inherent differences in the expression of protective sperm proteins in the fertile versus infertile group with high OS; 3) OS inducing oxidation of amino acid residue side chains, resulting in formation of carbonyl groups; 4) fragmentation of the polypeptide chain; and 5) the formation of protein-protein cross-linked aggregates. In the present study, the goal was to examine the oxidative stress–induced changes in sperm proteins with the use of proteomic tools in subjects who show high levels of ROS compared with those who do not. This may help to explain the differences in semen quality seen in infertile men who may exhibit no differences or have a significant overlap with fertile men (22) on evaluation by routine semen parameters. Therefore, the samples from each group were pooled based only on the ROS criteria, and the differential proteome between two pooled populations of sperm, i.e., sperm with high ROS level versus sperm with low ROS levels was investigated.

MATERIALS AND METHODS

After obtaining Institutional Review Board approval, semen samples from 20 donors and 32 infertile men were collected after 2–3 days of sexual abstinence and analyzed according to World Health Organization (WHO) 1999 criteria (23). Infertile subjects were evaluated for fertility and were referred by the urologist for a complete semen analysis. A complete semen analysis was performed on both donors and patients. Basic semen analysis included both macroscopic (volume, pH, color, viscosity, round cell concentration, liquefaction time, split or complete ejaculate) and microscopic parameters such as sperm concentration, motility and morphology, as well as peroxidase or Endtz test when the seminal leukocytes concentration was $>0.2 \times 10^6$/mL. Because of the nature of the study design, fresh samples were analyzed on their first visit for semen analysis and ROS. For this study, we only included semen parameters and levels of ROS and not any other clinical diagnosis. The remainder of the seminal ejaculate from each sample was frozen (and not cryopreserved in test yolk buffer) at −55°C and batched for proteomic analysis at a later time.

ROS levels in the seminal ejaculate were measured in each sample only in fresh samples using the luminol based chemiluminescence technique. Then, based on the cutoff value of 20 relative light units (RLU)/s/10^6 sperm, the semen samples were divided into two groups, namely, ROS+ and ROS−. Frozen samples were thawed, and semen samples of each group were pooled and centrifuged to separate spermatozoa from the seminal plasma. Sperm cell proteins were extracted and separated by 2D-DIGE. In-gel protein digestion was performed, followed by peptide separation with the use of liquid chromatography–mass spectrometer analysis (LC-MS) and identification of proteins with the use of Mascot, Sequest, and Blast search engines.

Semen Analysis

After liquefaction, manual semen analysis was performed with the use of a Microcell counting chamber (Vitrolife) to determine sperm concentration and percentage motility according to WHO guidelines (23). Viability was determined by eosin-nigrosin stain. Air-dried smears were stained with a Diff-Quik kit (Baxter Healthcare Corp.) for assessment of sperm morphology according to WHO criteria (23).

Measurement of Reactive Oxygen Species

ROS levels were measured by chemiluminescence assay with the use of luminol (5 mM; 5-amino-2, 3- dihydro-1, 4-phthalazinedione) and a luminometer (Autolumat LB 953) (24). Blanks and negative and positive control samples were run along with test samples. Blanks consisted of only 400 μL phosphate-buffered saline solution (PBS); negative control subjects were prepared by replacing semen with an equal volume of PBS and 10 μL luminol; positive samples contained 400 μL PBS, 50 μL hydrogen peroxide (37%), and 10 μL luminol. Test samples consisted of 400 μL semen and 10 μL luminol. Chemiluminescence was measured for 15 minutes, and results were expressed as RLU/s/10^6 sperm.

Spermatozoa Collection and Protein Extraction

Frozen semen samples from each study group (ROS+ and ROS−) were thawed and spermatozoa separated by centrifugation at 300*g* for 30 minutes at 4°C. Once the supernatant was removed, the spermatozoa from each study group (ROS+ and ROS−) were pooled and solubilized in lysis buffer containing 2% octyl-β-glucopyranoside, 100 mmol/L dithiothretol, 9.8 mol/L urea, and protease inhibitors. The spermatozoa samples were then stored overnight at 4°C to allow complete lysis of the spermatozoa, including the cell membranes. Acetonitrile was added to an aliquot of the lysed cells to precipitate the proteins. The proteins were then reconstituted in the CyDye labeling buffer (GE Healthcare). The concentration of protein was determined on a 5-μL aliquot with the use of the 2-D Quant kit (GE Healthcare). Aliquots of each protein were subsequently modified by CyDye labeling.

Sample Preparation and CyDye Labeling for Proteomic Studies

A small aliquot of each pooled sample was used to measure the protein concentration using the 2-D Quant kit (GE Healthcare); 50 μg of each sample was labeled with 400 pmol of either Cy3 or Cy5 at pH 8.5 for 30 minutes on ice. A Cy2-labeled internal standard (IS) was prepared by pooling 50 μg of each sample and labeling it with 400 pmol Cy2. Dye-swapping strategy was used in this experiment, by which the dyes used to label samples (Cy3 and Cy5) were swapped to run a duplicate gel to control for any dye-specific effects that might result from preferential labeling or different fluorescence characteristics of the gel at the different excitation wavelengths of Cy2, Cy3, and Cy5 (Supplemental Table 1, available online at www.fertstert.org). The duplicate gel provided additional data points for each group to conduct the Student *t* test for statistical analysis. The labeling reactions were stopped by addition of excess lysine to quench untreated N-hydroxysuccinimyl groups on the Cy Dyes. Equal amount of Cy2-labeled IS was loaded on each gel for normalization and to correct for gel-to-gel variability.

Two-Dimensional Differential In-Gel Electrophoresis

To detect protein differences between the two experimental conditions (i.e., ROS- vs. ROS+), a modified 2-D electrophoresis procedure was used. Equal amounts of the three Cy Dye–labeled samples were admixed, and Destreak sample buffer (GE Healthcare) containing 0.5% ampholytes (pH 3–10) was added to the mixture to a final volume of 200 μL. Each analytic gel was loaded with 150 μg total protein. Isoelectric focusing (IEF) was carried out on 11-cm Readystrip immobilized pH gradient (IPG) strips (pH 3–10 liner; Bio-Rad) with the use of the Protean IEF Cell (Bio-Rad). The sample (200 μL) was added to the IPG strip and actively rehydrated for 16 hours at 20°C with the use of 50 V and 50 μA/strip. IEF was carried out with the use of the following protocol: 1) rapid ramp to 250 V in 5 minutes; 2) rapid ramp to 8,000 V in 30 minutes; and 3) hold at 8,000 V for 4 hours 30 minutes. The current limit was set at 50 μA per strip and the temperature at 20°C. The strips were equilibrated for 15 minutes in a solution containing 6 mol/L urea, 30% glycerol, 2% sodium dodecyl sulfate, and 65 mmol/L dithiothreitol (DTT) followed by a second 15-minute equilibration with 25 mg/mL iodoacetamide instead of DTT. After equilibration, the 11-cm strips were fit into a Criterion 11-cm IPG gel and a standard SDS-PAGE second dimension was run. A Bio-Rad dual-color prestained Precision Plus Protein standard was run as the molecular weight marker.

Image Acquisition and Decyder Analysis

The CyDye–labeled gel was analyzed by post-run fluorescence imaging with the use of the Typhoon Trio Imager (GE Healthcare). The Cy2 images were acquired with a 488 nm excitation laser and a 520 nm emission filter; the Cy3 images used a 532 nm excitation laser with a 580 nm emission filter; and the Cy5 images were acquired with a 633 nm excitation laser and a 670 nm emission filter. The resolution was set to 100 μm. After the multiplexed images were acquired, image analysis was performed with the use of Decyder 5.01 software (GE Healthcare) using the "batch processor" module. After acquisition of the fluorescent image, the gel was stained with Gel Code Blue Coomassie stain (Thermo Scientific) for visualization purposes. Protein spots exhibiting ≥ 1.5-fold statistically significant ($P \leq .05$) difference in intensity between experimental groups were excised from the preparatory gel and identified by liquid chromatography–tandem mass spectrometry (LC-MS-MS; Finnigan LTQ).

In-Gel Digestion of Proteins

The uniquely identified spots were excised from the 2D-DIGE gels as closely as possible with a gel punch. They were then washed and destained in 50% acetonitrile containing 5% acetic acid followed by dehydration in the speed vac concentrator. The dried gel pieces were digested overnight with trypsin (5 μL of 10 ng/μL) in 50 mmol/L ammonium bicarbonate at 37°C. The peptides generated by trypsin digestion were extracted from the polyacrylamide gel in two 30-μL volumes of 50% acetonitrile and 5% formic acid. The extracts were combined and evaporated in a speed-vac concentrator to reduce the volume to 10 μL. The samples were resuspended in 1% acetic acid to make a final volume of ~30 μL for LC-MS analysis.

Liquid Chromatography–Tandem Mass Spectrometer Analysis

Ten-microliter volumes of the extracted peptide samples were injected on a Phenomenex Jupiter C18 reversed-phase capillary chromatography column (self-packed 9 cm × 75 μm inner diameter) for LC separation before introduction into online MS. The peptides eluted from the column by an acetonitrile plus 0.1% formic acid gradient at a flow rate of 0.25 μL/min were introduced into the MS source online. The MS system was a Finnigan LTQ linear ion trap MS system. The nanoelectrospray ion source was set to 2.5 kV. The digest was analyzed with the use of the data-dependent multitask capability of the instrument acquiring full-scan mass spectra to determine peptide molecular weights and product ion spectra to determine amino acid sequences in successive instrument scans.

Data Analysis

The data were analyzed with the use of all collision-induced dissociation (CID) spectra collected in the experiment by searching the National Center for Biotechnology Information (NCBI) human reference sequence database with the Mascot search engine (Matrix Science). Criteria for correct identifications were at least two matching peptide spectra with scores >40. The interpretation process was aided by additional searches using the Sequest and Blast programs as needed. The data were analyzed for differences in protein expression and their relevance to ROS generation.

RESULTS

Semen parameters in control and infertile men are presented in Table 1. ROS levels were significantly different in the ROS− and ROS+ groups [median (interquartile range [IQR]) RLU/s/10^6 sperm: 4 (0–9) vs. 2,236 (33–4,439; $P<.01$; Table 1]. The fluorescent images of the two gels with Cy3- and Cy5-labeled samples are shown in Figure 1A. The summary of the matching results of the two gels is shown in Supplemental Table 2 (available online at www.fertstert.org). A total of 1,343 protein spots in gel 1 and 1,265 spots in gel 2 were detected by the Decyder software aided by manual processing. The differential expression levels were compared by Decyder between the two groups by Student *t* test and then checked manually and confirmed individually.

The majority of protein spots (97.6%) were found to have similar expression levels, with a few spots (2.4%) showing >1.5-fold difference ($P<.05$). Table 2 lists 31 spots that were detected and were differentially expressed; of these, 6 spots decreased and 25 spots increased in abundance in the ROS− sample compared with the ROS+ sample. The positions of the 31 spots are circled on the 2-D gel in Figure 1B and marked with their spot numbers assigned by the Decyder software. The detailed information regarding each spot's change (fold increase) is given in Table 3. A total of 18 spots were marked as Pick in Table 3 and circled in red in Figure 1B. These spots were selected for further LC-MS-MS protein sequencing analysis owing to their abundance and position on the gel.

Eighteen spots were therefore cut from the 2D-DIGE gel. These spots were washed and digested with trypsin. The digests were analyzed by capillary-column LC-MS-MS and the CID spectra searched against the human reference sequence database. Each spot was positively identified with at least one protein. The proteins identified in each spot and the quantitative results from 2D-DIGE analysis are listed in Table 3. For spots that contained more than one protein, the major contributor to the observed quantitative abundance change was deduced based on relative abundance in the spots and the distribution of the proteins among several spots. The proteins thought to be most responsible for the observed differences are denoted by superscript a in Table 3.

Spot 143

The most abundant protein identified in spot 143 was A-kinase anchor protein (AKAP) 4 isoform 1 by the presence of ten peptides covering 15% of the protein sequence. Several additional proteins were also identified in this spot including heat shock protein (HSP) 90-β, AKAP3, fibronectin isoform 3 preprotein, and endoplasmin precursor. AKAP4, HSP 90-β, and endoplasmin precursor may be responsible for the observed difference in staining based on the abundance of the proteins in ROS+ samples.

Spot 183

Seven proteins were identified in this spot, the most abundant including HSP 90-α isoform 1, HSP 90-β, and lactotransferrin isoform 1 precursor. Based on the results from spot 143, HSP 90-β was the most likely candidate for the observed difference in staining, because it was highly expressed in ROS+ samples.

Spots 243, 250, 253, 257–259, and 263

These seven spots showed an increase in abundance in the ROS− sample. The most abundant protein identified in these

TABLE 1

Semen parameters in control subjects and patients as well as in ROS− and ROS+ groups.

Parameter	Control (n = 20)	Patient (n = 32)	ROS− (n = 21)	ROS+ (n = 31)
Sperm concentration	69.00 ± 42.96	42.90 ± 52.84	59.36 ± 45.61	43.5 ± 35.46
Motility (%)	55.00 ± 14.01	49.13 ± 16.42	51.85 ± 14.23	51.00 ± 16.74
Percentage normal morphology (Kruger strict criteria)	3.5 ± 1.6	3.6 ± 3.2	3.2 ± 2.5	3.8 ± 2.8
ROS (RLU/s/10^6 sperm)	368 ± 996.1	1,825 ± 4,781.2	1.32 ± 4.6	2,022 ± 5,680.9
Median (IQR)	2,219 (0–4,439)	282 (0–564)	4 (0–9)	2,236 (33–4,439)

Note: IQR = interquartile range; RLU = relative light unit; ROS = reactive oxygen species.

Hamada. Spermatozoa ROS and proteomic analysis. Fertil Steril 2013.

FIGURE 1

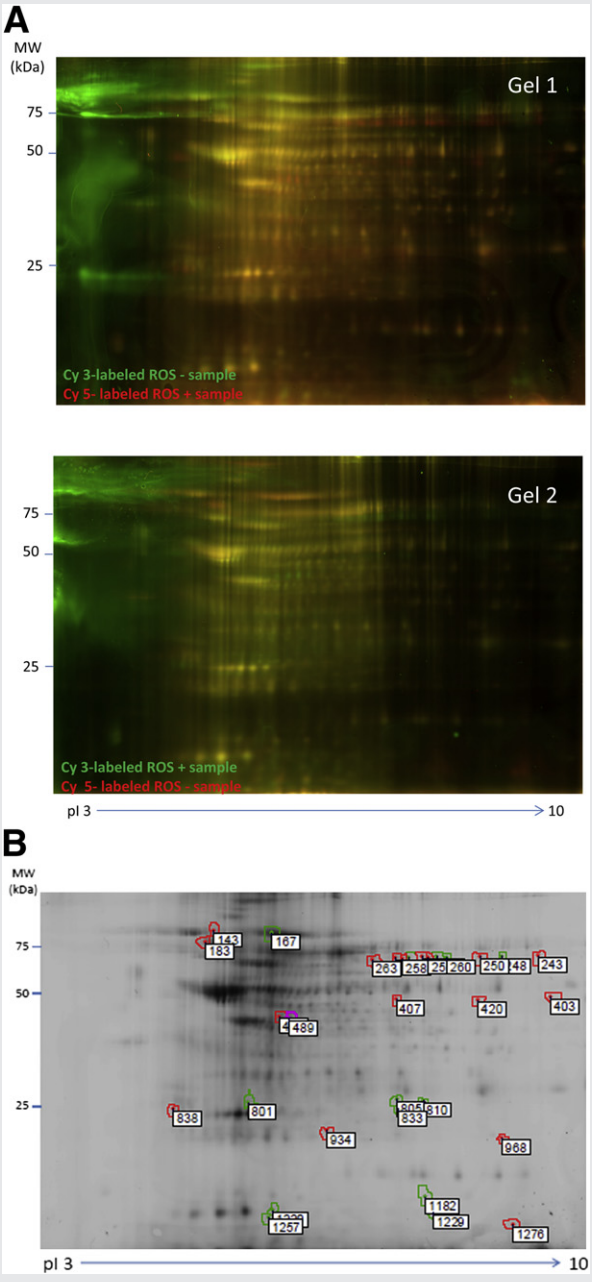

(A) Fluorescent images of the two-dimensional (2D) differential in-gel electrophoresis gels with Cy3- and Cy5-labeled samples. Dye swapping strategy was used, i.e., the dyes used to label samples (Cy3 and Cy5) were swapped to run a duplicate gel to control for any dye-specific effects that might result from preferential labeling or different fluorescence characteristics of the gel at the different excitation wavelengths of Cy2, Cy3, and Cy5. Gel 1: reactive oxygen species (ROS)–negative (ROS−) CY3 and ROS+ CY5; Gel 2: ROS− Cy5 and ROS+ Cy3. A Cy2-labeled internal standard was prepared by pooling 50 μg of each sample and labeling that pool with 400 pmol Cy2. (B) The positions of the 31 spots were circled on the 2D gel and marked with their respective spot numbers as assigned by Decyder software.

Hamada. Spermatozoa ROS and proteomic analysis. Fertil Steril 2013.

spots was lactotransferrin isoform 2, which was the only protein identified in spots 250, 258, 259, and 263.

TABLE 2

Differentially expressed proteins in human spermatozoa from ROS− versus ROS+ samples.

No.	Spot no.	Abundance of protein in ROS− sample	Ratio (fold increase/decrease) (ROS− vs. ROS+)	*P* value (*t* test)	Spot picked (Yes/No)
1	143	↓	−2.1	.022	Yes
2	183	↓	−2.33	.0035	Yes
3	243	↑	2.18	.00073	Yes
4	250	↑	2.57	.00017	Yes
5	253	↑	2.76	.03	Yes
6	257	↑	3.75	.031	Yes
7	258	↑	2.87	.037	Yes
8	259	↑	2.43	.037	Yes
9	263	↑	2.02	.049	Yes
10	403	↑	2.17	.0048	Yes
11	407	↑	2.06	.021	Yes
12	420	↑	2.57	.032	Yes
13	482	↑	3.04	.043	Yes
14	489	↑	2.2	.0065	Yes
15	838	↑	1.79	.0085	Yes
16	934	↑	1.6	.0015	Yes
17	968	↑	2.14	.0076	Yes
18	1,276	↓	−2.66	.022	Yes
19	167	↓	−2.22	.025	No
20	248	↑	2.06	.041	No
21	249	↑	1.87	.01	No
22	252	↑	2.1	.031	No
23	260	↑	2.27	.04	No
24	801	↑	1.63	.0017	No
25	805	↑	1.75	.024	No
26	810	↑	1.78	.01	No
27	833	↑	1.66	.039	No
28	1,182	↓	−1.98	.00018	No
29	1,220	↑	1.61	.0038	No
30	1,229	↓	−1.66	.00032	No
31	1,257	↑	1.83	.014	No

Hamada. Spermatozoa ROS and proteomic analysis. Fertil Steril 2013.

Spots 403, 407, and 420

These three protein spots were increased in the ROS− sample. The most abundant protein identified in these spots was lactotransferrin isoform 1 precursor, which was the only protein identified in spots 403 and 420.

Spots 482, 489, and 838

The most abundant protein identified in these three spots was tubulin β beta-4β chain by the presence of 8–28 peptides covering 18%–66% of the protein sequence. The results from the 2D-DIGE analysis indicated their increased presence in the ROS− sample. Several additional proteins were identified in these spots, and therefore the specific proteins responsible for the difference in CyDye labeling in these spots is unclear.

Spot 934

The most abundant proteins identified in this spot, which showed an increase in ROS−, were peroxiredoxin-1 by the presence of 8 peptides covering 44% of the protein sequence, manganese–superoxide dismutase (Mn-SOD) mitochondrial isoform A precursor by the presence of 3 peptides covering

TABLE 3

Summary, identification, and quantitative results of protein sequencing obtained from 2D-DIGE analysis.

Spot no.	Abundance (from 2D-DIGE)	Identification: Protein name	Calculated MW	NCBI database index number	Peptides (coverage)	Mascot score
143	Decreased in ROS−	A-kinase anchor protein 4 isoform 1[a]	95 kd, 6.8	21493037	10 (15%)	233
		Heat shock protein HSP 90-β[a]	83 kd, 4.9	20149594	3 (5%)	189
		A-kinase anchor protein 3	95 kd, 5.8	21493041	6 (7%)	179
		Fibronectin isoform 3 preproprotein	262 kd, 5.4	16933542	5 (2%)	108
		Endoplasmin precursor[a]	92 kd, 4.7	4507677	2 (2%)	89
183	Decreased in ROS−	Heat shock protein HSP 90-α isoform 1	98 kd, 5.0	153792590	15 (16%)	464
		Heat shock protein HSP 90-β[a]	83 kd, 4.9	20149594	10 (14%)	440
		Lactotransferrin isoform 1 precursor	80 kd, 8.5	54607120	11 (23%)	412
		A-kinase anchor protein 4 isoform 1	95 kd, 6.8	21493037	1 (2%)	87
		Endoplasmin precursor	92 kd, 4.7	4507677	3 (4%)	87
		Fibronectin isoform 3 preproprotein	262 kd, 5.4	16933542	3 (1%)	76
		A-kinase anchor protein 3	95 kd, 5.8	21493041	2 (2%)	64
243	Increased in ROS−	Lactotransferrin isoform 2[a]	74 kd, 8.2	312433998	— (50%)	986
		Trifunctional enzyme subunit α, mitochondrial precursor	83 kd, 9.1	20127408	3 (9%)	186
		Glyceraldehyde-3-phosphate dehydrogenase, testis-specific	44 kd, 8.3	7657116	2 (6%)	71
250	Increased in ROS−	Lactotransferrin isoform 2[a]	74 kd, 8.2	312433998	— (43%)	1,209
253	Increased in ROS−	Lactotransferrin isoform 2[a]	74 kd, 8.2	312433998	25 (47%)	1,066
		Glyceraldehyde-3-phosphate dehydrogenase, testis-specific	44 kd, 8.3	7657116	1 (3%)	65
257	Increased in ROS−	Lactotransferrin isoform 2[a]	74 kd, 8.2	312433998	30 (54%)	2,301
		Trifunctional enzyme subunit α, mitochondrial precursor	83 kd, 9.1	20127408	6 (11%)	138
		A-kinase anchor protein 4 isoform 1	95 kd, 6.8	21493037	2 (3%)	122
		Glyceraldehyde-3-phosphate dehydrogenase, testis-specific	44 kd, 8.3	7657116	2 (5%)	107
		Pyruvate kinase isozymes M1/M2 isoform c	66 kd, 7.9	332164775	4 (7%)	64
258	Increased in ROS−	Lactotransferrin isoform 2[a]	74 kd, 8.2	312433998	10 (18%)	321
259	Increased in ROS−	Lactotransferrin isoform 2[a]	74 kd, 8.2	312433998	— (44%)	834
263	Increased in ROS−	Lactotransferrin isoform 2[a]	74 kd, 8.2	312433998	9 (18%)	409
403	Increased in ROS−	Lactotransferrin isoform 1 precursor	80 kd, 8.5	54607120	4 (7%)	164
407	Increased in ROS−	Lactotransferrin isoform 1 precursor	80 kd, 8.5	54607120	10 (17%)	472
		Glyceraldehyde-3-phosphate dehydrogenase, testis-specific	44 kd, 8.3	7657116	3 (9%)	94
420	Increased in ROS−	Lactotransferrin isoform 1 precursor	80 kd, 8.5	54607120	7 (14%)	240
482	Increased in ROS−	Tubulin β-4B chain	50 kd, 4.8	5174735	25 (65%)	2,339
		tubulin β-4A chain	50 kd, 4.7	21361322	18 (52%)	1,796
		Succinyl-CoA ligase [ADP-forming] subunit β, mitochondrial precursor	50 kd, 7.0	11321583	9 (20%)	294
		Actin, cytoplasmic 1	42 kd, 5.2	4501885	9 (30%)	263
		Creatine kinase B-type	42 kd, 5.3	21536286	3 (9%)	182
		Lactotransferrin isoform 1 precursor	80 kd, 8.5	54607120	5 (8%)	154
		Desmoplakin isoform I	334 kd, 6.4	58530840	8 (2%)	153
		Outer dense fiber protein 2 isoform 8	67 kd, 7.3	334278918	4 (6%)	117
		A-kinase anchor protein 4 isoform 1	95 kd, 6.8	21493037	3 (5%)	108
489	Increased in ROS−	Tubulin β-4B chain	50 kd, 4.8	5174735	28 (66%)	2,553
		Medium-chain specific acyl-CoA dehydrogenase, mitochondrial isoform a precursor	47 kd, 8.6	4557231	8 (22%)	250
		Actin, cytoplasmic 1	42 kd, 5.3	4501885	6 (24%)	232

Hamada. Spermatozoa ROS and proteomic analysis. Fertil Steril 2013.

TABLE 3

Continued.

Spot no.	Abundance (from 2D-DIGE)	Protein name	Identification: Calculated MW	Identification: NCBI database index number	Identification: Peptides (coverage)	Identification: Mascot score
		Isocitrate dehydrogenase [NADP] cytoplasmic	46 kd, 6.5	28178825	3 (12%)	138
		Pyruvate kinase isozymes M1/M2 isoform a	58 kd, 7.9	33286418	3 (7%)	128
		Adenosylhomocysteinase isoform 2	45 kd, 6.0	239937451	4 (13%)	121
838	Increased in ROS−	Tubulin β-4B chain	50 kd, 4.8	5174735	8 (18%)	973
		Proteasome subunit α type-5 isoform	26 kd, 4.7	23110942	10 (46%)	488
		Eukaryotic translation initiation factor 6 isoform a	27 kd, 4.5	4504771	4 (22%)	193
		Heat shock protein HSP 90-β (truncated?)	83 kd, 4.9	20149594	2 (3%)	128
		A-kinase anchor protein 4 isoform 1 (truncated?)	95 kd, 6.8	21493037	2 (2%)	85
		A-kinase anchor protein 3	95 kd, 5.8	21493041	2 (2%)	85
934	Increased in ROS−	Peroxiredoxin-1[a]	22 kd, 8.2	4505591	8 (44%)	205
		Superoxide dismutase [Mn], mitochondrial isoform A precursor[a]	24 kd, 8.3	67782305	3 (13%)	153
		Sorbitol dehydrogenase	38 kd, 8.2	156627571	1 (4%)	125
		Ras-related protein Rab-2A isoform a	23 kd, 6.0	4506365	1 (6%)	119
		SPRY domain−containing protein 7 isoform 1	22 kd, 6.2	20531765	2 (13%)	102
		Semenogelin-2 precursor[a]	65 kd, 9.0	4506885	3 (6%)	85
		Semenogelin-1 preproprotein	52 kd, 9.3	4506883	4 (8%)	83
		Heat shock protein β-1	22 kd, 5.9	4504517	2 (12%)	72
		Elongation factor 1-α1	50 kd, 9.1	4503471	3 (7%)	68
968	Increased in ROS−	Glyceraldehyde-3-phosphate dehydrogenase, testis-specific[a]	4 kd, 8.38	7657116	2 (6%)	88
1,276	Decreased in ROS−	Semenogelin-1 preproprotein	52 kd, 9.3	4506883	10 (19%)	441
		Semenogelin-2 precursor	65 kd, 9.0	4506885	4 (6%)	206
		Sperm protein associated with the nucleus on the X chromosome C	11 kd, 5.0	13435137	1 (11%)	94

Note: 2D-DIGE = two-dimensional differential in-gel electrophoresis; MW = molecular weight; NCBI = National Center for Biotechnology Information; ROS = reactive oxygen species.

[a] Most abundant proteins per spot.

Hamada. Spermatozoa ROS and proteomic analysis. Fertil Steril 2013.

13% of the protein sequence, and semenogelin (Sg) 2 precursor with three peptides and covering 6%.

Spot 968

Glyceraldehyde-3-phosphate dehydrogenase (GADH) , a testis-specific enzyme, was the only protein in this spot, which showed an increase in ROS−, and was identified by the presence of two peptides covering 6% of the protein sequence. GADH was also abundant in spots 243, 253, and 257, which also showed an increase in abundance in the ROS− group.

Spot 1,276

The two most abundant proteins identified in this spot, which showed a reduction in ROS− group, were Sg-1 preprotein and Sg-2 precursor.

DISCUSSION

In this novel study, we compared the differential protein expression in pooled spermatozoa from semen samples with high ROS with those with low ROS levels with the use of 2D-DIGE and MS. As the most important factor that leads to inaccuracy in the results is the gel variability, the 2D-DIGE was selected to run different samples on the same gel to reduce such variability. Furthermore, to eliminate fluorescence dye–specific effects due to preferential labeling or different fluorescence characteristics of the gel at the different excitation wavelengths of Cy2, Cy3, and Cy5, dye swapping was used in this experiment. We showed a total of 1,343 protein spots in gel 1 (ROS−) and 1,265 spots in gel 2 (ROS+), detected by Decyder software aided by manual processing. Although the majority of protein spots (97.6%) had similar expression pattern, 31 spots (2.4%) showed a significant difference ($P<.05$) of ≥ 1.5-fold. Six spots decreased and 25 increased in abundance in the ROS− sample compared with the ROS+ sample. Eighteen spots were picked for further LC-MS-MS analysis for protein sequencing based on the observed statistical differences in the spots, which revealed that eight proteins were responsible for the differences in the protein spots.

The most abundant protein identified in spots 143 and 183 was AKAP4 (peptide coverage [PC] 15% and 4%, respectively). Several additional proteins were also identified in these spots, including HSP 90-β (PC 5% and 14%), AKAP3 (PC 7% and 2%), fibronectin (PC 2%, 1%, and 2%), and endoplasmin (PC 2% and 4%). The three major proteins that are highly expressed in spermatozoa in semen samples with OS and are responsible for the observed difference in staining based on the abundance of the proteins include AKAP4, HSP 90-β, and endoplasmin.

AKAP4 (82 kd) is a cytoskeletal phosphoprotein that constitutes about one-half of the proteinaceous components of the fibrous sheath in mouse sperm (25). AKAP4 plays an important role in sperm motility because it anchors protein kinase A, which can, under high cyclic adenosine monophosphate (cAMP) stimulation, phosphorylate other functional proteins (26–28). High ROS levels can lead to high cAMP and tyrosine phosphorylation of AKAP4 (29, 30). This phosphorylation may explain the differential abundance of AKAP4 in sperm with high OS. Moreover, high ROS levels can induce premature capacitation, which leads to increased levels of AKAP4 phosphorylation, as reported by Ficarro et al. (31). Kriegel et al. reported a 3.41-fold increase of AKAP4 in sperm of men with type 1 diabetes (OS-inducing conditions) compared with sperm from healthy men (32).

HSPs, also known as stress proteins, are a family of proteins that constitute 5%–10% of all cellular proteins and aid in protein translocation, folding, and assembly under normal cellular conditions (33). In response to cellular stressors, such as heat, glucose deprivation, free radical attack, and infection, they are overexpressed (34–36). This reactive response can explain the increase in HSP 90-β and endoplasmin HSP 90-β1 in sperm with high ROS levels.

HSP 90-β possesses three thiol groups, which can participate in reduction of cytochrome C (apoptotic signal) and protect the cells from apoptosis (37). However, excessively oxidized SH groups and S-nitrosylation result in loss of its chaperon activity and increase in molecular weight (38).

In ROS− sperm, overabundance of four antioxidant proteins have been identified that may exert essential cytoprotective effects against the build-up of ROS levels. These proteins are lactotransferrin isoform 2, lactotransferrin isoform 1 precursor, peroxiredoxin-1, and Mn-SOD mitochondrial isoform A precursor.

Lactotransferrin isoform 2 was abundant in seven spots (spots 243, 250, 253, 257, 258, 259, and 263) from the ROS− sample. This protein was the sole protein identified in four spots, namely, 250, 258, 259, and 263. Lactotransferrin isoform 1 was identified in three spots (403, 407, and 420) that were also increased in abundance in the ROS− sample. Lactotransferrin isoform 1 precursor was the sole protein to be identified in spots 403 and 420.

Lactoferrin (80 kd), also known as lactotransferrin, is a non-heme iron-binding epididymal glycoprotein that adheres to the sperm surface and acts as an antioxidant, antibacterial, and immune-modulating agent (39–42). Kruzel et al. showed in experiments on nontumorigenic parenchymal liver cells that the lactoferrin isoform can protect the cells from the mitochondrial oxidative burst induced by exposure to lipopolysaccharide (43). Iron is an essential catalyst for the ROS production as it immediately reacts with H_2O_2, thereby producing highly reactive OH (Fenton/Haber-Weiss biochemical pathway) (44). Thus, lactoferrin-chelating effects on iron can reduce the production of harmful levels of ROS and counteract their lipid peroxidation effects.

Spot 934 showed the preponderance of two proteins, namely, peroxiredoxin-1 with 44% peptide coverage and Mn-SOD, mitochondrial isoform A precursor with 13% peptide coverage. Abundance of Sg-2 precursor was seen in this spot and spot 1,276, which also showed abundance of Sg-1 precursor.

Peroxiredoxins (PRDXs) are selenium-free and heme-free peroxidases with molecular weights ranging from 22 to 31 kd (45, 46). PRDXs detoxify H_2O_2 similarly to catalases or glutathione peroxidases (GPXs) (18, 45, 47). They are characterized by their abundant cellular distribution and presence compared with catalase and GPX (47, 48). PRDX1 has two cysteine residues and is able to react with H_2O_2. In

sperm, PRDX1 is located on the tail, the equatorial segment, and postacrosomal region of the head (49). O'Flaherty et al. confirmed by means of an in vitro study that sperm PRDX 1 expression is reduced in response to H_2O_2 in a dose-dependent manner (49). This might explain our results, which showed lower expression of PRDX1 among sperm samples with high ROS levels.

SOD is a metal-binding protein which protects cells from ROS by scavenging superoxide radicals by converting them into H_2O_2, which in turn is detoxified by PRDX, GPX, and catalase. Two forms of intracellular forms of SOD are localized to the mitochondria (Mn-SOD) and to the cytoplasm (Cu/Zn-SOD). Our results showed higher Mn-SOD (mitochondrial isoform A precursor, 24 kd, pI [isoelectric point] 8.3) expression in sperm from semen with low ROS production versus sperm obtained from men with high ROS levels. Our results are in agreement with those of Aly et al., who demonstrated in an in vitro experiment on sperm mitochondria that on exposure to lipopolysaccharide, oxidative markers such as H_2O_2 and MDA increased whereas a significant reduction in the Mn-SOD activity was noticed (50). Agarwal et al. showed lower levels of intracellular sperm SOD in infertile men with asthenospermia and high levels of OS (51).

Semenogelin-2 precursor and Sg-1 preprotein showed overabundance in ROS− samples in a single spot (spot 934). Because this spot was reduced in ROS− samples, and Sg-1 preprotein and Sg-2 precursor were shown to be increased in multiple ROS− spots, the results may indicate that the isoform patterns of the Sg-1 proteins may differ between the ROS− and ROS+ samples (see spot 934). Further experiments will need to be performed to verify this.

Semenogelin is the major protein of seminal fluid proteins (20%–40%) and is secreted from the seminal vesicles, epididymis, and prostate (52, 53). It is an androgen-dependent protein that exists in forms: I (52 kd) and II (71–76 kd). These two forms perform similar physiologic functions. They are encoded by genes on the long arm of chromosome 20 and share similar repeats of 60 amino acids. Sg helps in formation of the semen coagulum that is degraded later by prostatic-specific antigen. After degradation, Sg is cleaved into several peptides that are either adsorbed on the spermatozoon surface or internalized to regulate important physiologic pathways (54, 55). Reversible inhibition of sperm motility and premature activation of capacitation of ejaculated sperm are the two main functions (55).

In addition to combating OS, Sg can reduce generation of free radicals through several mechanisms:

1. Slow sperm motility of the entrapped sperm and reduce energy consumption and free radical generation (56).
2. Inhibit superoxide radical generation through direct interference with sperm NADH oxidase (57).
3. Sg usually binds to high amounts of zinc (zinc has antioxidant and anticapacitating effects) and sequesters it to act on and inside the spermatozoa (57).

GADH, the testis-specific protein identified in spot 968, was abundant in ROS− sperm samples (PC 6%) versus ROS+. This finding might be attributed to ROS-induced degradation of this glycolytic enzyme. GADH is an important glycolytic enzyme with a single active thiol (cysteine) group (58). This enzyme is essential for male fertility, because knockout mice for this gene are sterile (59). Although oxidation by superoxide and nitric oxide at the thiol group was found to reduce the enzyme activity, no studies have measured its exact intracellular levels after oxidation (60, 61). Bailey et al. showed reduced in vitro intracellular levels of this enzyme 3–5 days after exposure in aging muscle with the use of an ischemia-reperfusion model (OS-inducing model) (62).

The findings from the present study broaden the proteome spectrum of the sperm and identifies a subset of the sperm proteome, which may be implicated in genesis of OS. Moreover, several of these markers can serve as molecular biomarkers to show the differences between the physiologically normal intact sperm and those with high oxidant burden.

It may be important to mention here that we measured ROS levels only in the fresh samples and grouped these into ROS+ and ROS− groups, which were subsequently frozen. Proteomic analysis was performed after thawing these samples. We did not examine if any differences in the protein profile found between donors and patients with different ROS levels in the fresh aliquots could be attributed to a differential semen behavior as a result of freezing before performing the proteomic analysis. Another limitation of this study was the inability to confirm whether differentially expressed proteins are OS related or are OS-modified proteins. Revalidation of the results by quantitative Western immunoblot analysis of sperm extracts with specific antibodies is important. However, this was a pilot study for proof of concept. Quantitative estimation of the differentially expressed proteins is important to identify the proteins represented in the study using Western blotting and antibodies against these proteins. Although it is difficult to quantify the large number of proteins that are differentially expressed in our study groups, we examined our 2D-DIGE data and identified two proteins as the best candidates. The first protein is lactotransferrin-2 (NCBI #312433998). It is invariably present in multiple spots (Table 3). The second protein is peroxiredoxin-1 (NCBI #4505591). The 2D-DIGE data suggest that both of these proteins are increased in the ROS− group. We plan to quantify these proteins in our ongoing series of investigation.

In conclusion, the inherent intracellular and extracellular content of antioxidants determines the susceptibility of spermatozoa to OS. Adequate amount of antioxidants can protect the spermatozoa from damage, whereas low amounts may render the spermatozoa vulnerable to ROS attack. Furthermore, OS can induce or inhibit synthesis of particular proteins and can oxidatively modify intracellular proteins in different ways, e.g., increase in molecular weight, aggregation, or proteolysis.

Acknowledgments: The authors thank Ms. Dongmei Zhang for her assistance in analyzing the samples for proteomic study.

REFERENCES

1. Lewis SE, Boyle PM, McKinney KA, Young IS, Thompson W. Total antioxidant capacity of seminal plasma is different in fertile and infertile men. Fertil Steril 1995;64:868–70.

2. de Lamirande E, Jiang H, Zini A, Kodama H, Gagnon C. Reactive oxygen species and sperm physiology. Rev Reprod 1997;2:48–54.
3. Sikka SC. Relative impact of oxidative stress on male reproductive function. Curr Med Chem 2001;8:851–62.
4. Agarwal A, Prabakaran S, Allamaneni S. What an andrologist/urologist should know about free radicals and why. Urology 2006;67:2–8.
5. Agarwal A, Makker K, Sharma R. Clinical relevance of oxidative stress in male factor infertility: an update. Am J Reprod Immunol 2008;59:2–11.
6. de Lamirande E, Gagnon C. Impact of reactive oxygen species on spermatozoa: a balancing act between beneficial and detrimental effects. Hum Reprod 1995;10:15–21.
7. Aitken RJ, Paterson M, Fisher H, Buckingham DW, van Duin M. Redox regulation of tyrosine phosphorylation in human spermatozoa and its role in the control of human sperm function. J Cell Sci 1995;108:2017–25.
8. Zini A, de Lamirande E, Gagnon C. Low levels of nitric oxide promote human sperm capacitation in vitro. J Androl 1995;16:424–31.
9. Cocuzza M, Athayde KS, Agarwal A, Sharma R, Pagani R, Lucon AM, et al. Age-related increase of reactive oxygen species in neat semen in healthy fertile men. Urology 2008;71:490–4.
10. Venkatesh S, Riyaz AM, Shamsi MB, Kumar R, Gupta NP, Mittal S, et al. Clinical significance of reactive oxygen species in semen of infertile Indian men. Andrologia 2009;41:251–6.
11. Alvarez JG, Storey BT. Assessment of cell damage caused by spontaneous lipid peroxidation in rabbit spermatozoa. Biol Reprod 1984;30:323–31.
12. Storey BT. Biochemistry of the induction and prevention of lipoperoxidative damage in human spermatozoa. Mol Hum Reprod 1997;3:203–13.
13. Jones R, Mann T, Sherins R. Peroxidative breakdown of phospholipids in human spermatozoa, spermicidal properties of fatty acid peroxides, and protective action of seminal plasma. Fertil Steril 1979;31:531–7.
14. Aitken RJ, Clarkson JS. Cellular basis of defective sperm function and its association with the genesis of reactive oxygen species by human spermatozoa. J Reprod Fertil 1987;81:459–69.
15. Das S, Chattopadhyay R, Jana SK, Narendra BK, Chakraborty C, Chakravarty B, et al. Cut-off value of reactive oxygen species for predicting semen quality and fertilization outcome. Syst Biol Reprod Med 2008;54:47–54.
16. Tremellen K. Oxidative stress and male infertility—a clinical perspective. Hum Reprod Update 2008;14:243–58.
17. Rabilloud T, Chevallet M, Luche S, Leize-Wagner E. Oxidative stress response: a proteomic view. Expert Rev Proteomics 2005;2:949–56.
18. Rabilloud T, Heller M, Gasnier F, Luche S, Rey C, Aebersold R, et al. Proteomics analysis of cellular response to oxidative stress. Evidence for in vivo overoxidation of peroxiredoxins at their active site. J Biol Chem 2002;277:19396–401.
19. Baker MA, Witherdin R, Hetherington L, Cunningham-Smith K, Aitken RJ. Identification of post-translational modifications that occur during sperm maturation using difference in two-dimensional gel electrophoresis. Proteomics 2005;5:1003–12.
20. Aguilar-Mahecha A, Hales BF, Robaire B. Expression of stress response genes in germ cells during spermatogenesis. Biol Reprod 2001;65:119–27.
21. Aitken RJ, Baker MA. The role of proteomics in understanding sperm cell biology. Int J Androl 2008;31:295–302.
22. Agarwal A, Sharma RK, Nallella KP, Thomas AJ Jr, Alvarez JG, Sikka SC. Reactive oxygen species as an independent marker of male factor infertility. Fertil Steril 2006;86:878–85.
23. World Health Organization. WHO laboratory manual for the examination and processing of human semen. 4th ed. Geneva: World Health Organization; 1999.
24. Agarwal A, Allamaneni SS, Said TM. Chemiluminescence technique for measuring reactive oxygen species. Reprod Biomed Online 2004;9:466–8.
25. Miki K, Willis WD, Brown PR, Goulding EH, Fulcher KD, Eddy EM. Targeted disruption of the Akap4 gene causes defects in sperm flagellum and motility. Dev Biol 2002;248:331–42.
26. Edwards AS, Scott JD. A-Kinase anchoring proteins: protein kinase A and beyond. Curr Opin Cell Biol 2000;12:217–21.
27. Dodge K, Scott JD. AKAP79 and the evolution of the AKAP model. FEBS Lett 2000;476:58–61.
28. Brown PR, Miki K, Harper DB, Eddy EM. A-Kinase anchoring protein 4 binding proteins in the fibrous sheath of the sperm flagellum. Biol Reprod 2003;68:2241–8.
29. Ford WC. Regulation of sperm function by reactive oxygen species. Hum Reprod Update 2004;10:387–99.
30. Aitken RJ, Harkiss D, Knox W, Paterson M, Irvine DS. A novel signal transduction cascade in capacitating human spermatozoa characterised by a redox-regulated, cAMP-mediated induction of tyrosine phosphorylation. J Cell Sci 1998;111:645–56.
31. Ficarro S, Chertihin O, Westbrook VA, White F, Jayes F, Kalab P, et al. Phosphoproteome analysis of capacitated human sperm. Evidence of tyrosine phosphorylation of a kinase-anchoring protein 3 and valosin-containing protein/p97 during capacitation. J Biol Chem 2003;278:11579–89.
32. Kriegel TM, Heidenreich F, Kettner K, Pursche T, Hoflack B, Grunewald S, et al. Identification of diabetes- and obesity-associated proteomic changes in human spermatozoa by difference gel electrophoresis. Reprod Biomed Online 2009;19:660–70.
33. Pockley AG. Heat shock proteins as regulators of the immune response. Lancet 2003;362:469–76.
34. Sung DY, Guy CL. Physiological and molecular assessment of altered expression of Hsc70-1 in *Arabidopsis*. Evidence for pleiotropic consequences. Plant Physiol 2003;132:979–87.
35. Feder ME, Hofmann GE. Heat-shock proteins, molecular chaperones, and the stress response: evolutionary and ecological physiology. Annu Rev Physiol 1999;61:243–82.
36. Katschinski DM. On heat and cells and proteins. News Physiol Sci 2004;19:11–5.
37. Nardai G, Sass B, Eber J, Orosz G, Csermely P. Reactive cysteines of the 90-kda heat shock protein, Hsp90. Arch Biochem Biophys 2000;384:59–67.
38. Gao C, Guo H, Wei J, Mi Z, Wai PY, Kuo PC. Identification of S-nitrosylated proteins in endotoxin-stimulated RAW264.7 murine macrophages. Nitric Oxide 2005;12:121–6.
39. Salamah AA, al-Obaidi AS. Effect of some physical and chemical factors on the bactericidal activity of human lactoferrin and transferrin against *Yersinia pseudotuberculosis*. New Microbiol 1995;18:275–81.
40. Legrand D, Elass E, Carpentier M, Mazurier J. Lactoferrin: a modulator of immune and inflammatory responses. Cell Mol Life Sci 2005;62:2549–59.
41. Arnold RR, Cole MF, McGhee JR. A bactericidal effect for human lactoferrin. Science 1977;197:263–5.
42. Ward PP, Paz E, Conneely OM. Multifunctional roles of lactoferrin: a critical overview. Cell Mol Life Sci 2005;62:2540–8.
43. Kruzel ML, Actor JK, Radak Z, Bacsi A, Saavedra-Molina A, Boldogh I. Lactoferrin decreases LPS-induced mitochondrial dysfunction in cultured cells and in animal endotoxemia model. Innate Immun 2010;16:67–79.
44. Kehrer JP. The Haber-Weiss reaction and mechanisms of toxicity. Toxicology 2000;149:43–50.
45. Rhee SG, Chae HZ, Kim K. Peroxiredoxins: a historical overview and speculative preview of novel mechanisms and emerging concepts in cell signaling. Free Radic Biol Med 2005;38:1543–52.
46. Wood ZA, Schroder E, Robin Harris J, Poole LB. Structure, mechanism and regulation of peroxiredoxins. Trends Biochem Sci 2003;28:32–40.
47. Wood ZA, Poole LB, Karplus PA. Peroxiredoxin evolution and the regulation of hydrogen peroxide signaling. Science 2003;300:650–3.
48. Immenschuh S, Baumgart-Vogt E, Tan M, Iwahara S, Ramadori G, Fahimi HD. Differential cellular and subcellular localization of heme-binding protein 23/peroxiredoxin I and heme oxygenase-1 in rat liver. J Histochem Cytochem 2003;51:1621–31.
49. O'Flaherty C, de Souza AR. Hydrogen peroxide modifies human sperm peroxiredoxins in a dose-dependent manner. Biol Reprod 2010;84:238–47.
50. Aly HA, el-Beshbishy HA, Banjar ZM. Mitochondrial dysfunction induced impairment of spermatogenesis in LPS-treated rats: modulatory role of lycopene. Eur J Pharmacol 2012;677:31–8.
51. Agarwal A, Nallella KP, Allamaneni SS, Said TM. Role of antioxidants in treatment of male infertility: an overview of the literature. Reprod Biomed Online 2004;8:616–27.

52. Lilja H, Lundwall A. Molecular cloning of epididymal and seminal vesicular transcripts encoding a semenogelin-related protein. Proc Natl Acad Sci U S A 1992;89:4559–63.
53. Lilja H, Abrahamsson PA, Lundwall A. Semenogelin, the predominant protein in human semen. Primary structure and identification of closely related proteins in the male accessory sex glands and on the spermatozoa. J Biol Chem 1989;264:1894–900.
54. Jarow JP. Semenogelin, the main protein of semen coagulum, inhibits human sperm capacitation by interfering with the superoxide anion generated during this process. J Urol 2002;168:2309–10.
55. de Lamirande E. Semenogelin, the main protein of the human semen coagulum, regulates sperm function. Semin Thromb Hemost 2007;33:60–8.
56. de Lamirande E, Yoshida K, Yoshiike TM, Iwamoto T, Gagnon C. Semenogelin, the main protein of semen coagulum, inhibits human sperm capacitation by interfering with the superoxide anion generated during this process. J Androl 2001;22:672–9.
57. Bonilha VL, Rayborn ME, Shadrach KG, Li Y, Lundwall A, Malm J, et al. Semenogelins in the human retina: differences in distribution and content between AMD and normal donor tissues. Exp Eye Res 2008;86: 150–6.
58. Nakajima H, Amano W, Fujita A, Fukuhara A, Azuma YT, Hata F, et al. The active site cysteine of the proapoptotic protein glyceraldehyde-3-phosphate dehydrogenase is essential in oxidative stress-induced aggregation and cell death. J Biol Chem 2007;282:26562–74.
59. Miki K, Qu W, Goulding EH, Willis WD, Bunch DO, Strader LF, et al. Glyceraldehyde 3-phosphate dehydrogenase-S, a sperm-specific glycolytic enzyme, is required for sperm motility and male fertility. Proc Natl Acad Sci U S A 2004;101:16501–6.
60. Souza JM, Radi R. Glyceraldehyde-3-phosphate dehydrogenase inactivation by peroxynitrite. Arch Biochem Biophys 1998;360:187–94.
61. Elkina YL, Atroshchenko MM, Bragina EE, Muronetz VI, Schmalhausen EV. Oxidation of glyceraldehyde-3-phosphate dehydrogenase decreases sperm motility. Biochemistry (Mosc) 2011;76:268–72.
62. Bailey CE, Hammers DW, Deford JH, Dimayuga VL, Amaning JK, Farrar R, et al. Ishemia-reperfusion enhances GAPDH nitration in aging skeletal muscle. Aging (Albany NY) 2011;3:1003–17.

SUPPLEMENTAL TABLE 1

Summary of samples and experimental design.

Sample no.	Description	Original protein concentration ($\mu g/\mu L$)	Cy Dye label	2D-DIGE gel no.
1	ROS−	11.21	Cy3	1
2	ROS+	10.59	Cy5	1
1	ROS−	11.21	Cy5	2
2	ROS+	10.59	Cy3	2
Internal standards (2 × 50 μg)	—	—	Cy2	1 and 2

Note: 2D-DIGE = two-dimensional differential in-gel electrophoresis; ROS = reactive oxygen species.

Hamada. Spermatozoa ROS and proteomic analysis. Fertil Steril 2013.

SUPPLEMENTAL TABLE 2

Summary of matching results of 2D-DIGE analysis.

Status	Image	Label	No. of spots	Matched	Group	Group description
Master	Gel 1 scan 2 standard CY2	Cy2	1343	1343	Standard	—
Matched	Gel 1 scan 2 Cy3.gel	Cy3	1343	1343	ROS−	Sample1
Matched	Gel 1 scan 2 Cy5.gel	Cy5	1343	1343	ROS+	Sample 2
Matched	Gel 2 scan 2 standard CY2	Cy2	1265	957	Standard	—
Matched	Gel 2 scan 2 Cy3.gel	Cy3	1265	957	ROS+	Sample 2
Matched	Gel 2 scan 2 Cy5.gel	Cy5	1265	957	ROS−	Sample 1

Note: 2D-DIGE = two-dimensional differential in-gel electrophoresis; ROS = reactive oxygen species.

Hamada. Spermatozoa ROS and proteomic analysis. Fertil Steril 2013.